agriculture

MDPI

Article

Stability of Maize Phenology Predictions by Using Calendar Days, Thermal Functions, and Photothermal Functions

Yen-Yu Liu [1,†], Yuan-Chih Su [1,†], Ping-Wei Sun [2], Hung-Yu Dai [2] and Bo-Jein Kuo [1,3,*]

[1] Department of Agronomy, National Chung Hsing University, 145 Xingda Rd., South Dist., Taichung City 40227, Taiwan; d108031001@mail.nchu.edu.tw (Y.-C.S.)
[2] Crop Science Division, Taiwan Agricultural Research Institute, Ministry of Agriculture, 189 Zhongzheng Rd., Wufeng Dist., Taichung City 413008, Taiwan; pwsun@tari.gov.tw (P.-W.S.); hydai@tari.gov.tw (H.-Y.D.)
[3] Smart Sustainable New Agriculture Research Center (SMARTer), Taichung 40227, Taiwan
* Correspondence: bjkuo@dragon.nchu.edu.tw; Tel.: +886-4-22840777 (ext. 201)
† These authors contributed equally to this work.

Abstract

Accurate prediction of crop phenological stages is essential for effective crop management. Such a prediction provides the timing of phenological stages, thus aiding in scheduling management practices, understanding the potential risks of adverse weather at critical phenological stages, and adjusting sowing dates. Temperature is the dominant climatic factor affecting maize (*Zea mays* L.) development, with photoperiod serving as a secondary influence. This study used maize field data with recorded flowering and maturity dates to evaluate the stability of phenological stage predictions obtained using the calendar days method, thermal functions, and photothermal functions. These methods were used to calculate the number of days, accumulated temperature, and accumulated photothermal units from sowing to flowering and from flowering to maturity. Results showed that thermal functions produced the most stable predictions, with the lowest average coefficient of variation (CV) being 8.37%. The thermal functions were further categorized as empirical linear, empirical nonlinear, and process-based. Within each category, the functions with the lowest average CVs were growing degree days ($GDD_{8,34}$; 9.12%), thermal leaf unit (GTI; 7.74%), and agricultural production system simulator (APSIM; 8.26%), respectively. Among them, GTI had the lowest CV, indicating its superior stability in predicting maize phenological stages. These results provide a basis for selecting thermal models in maize phenology research and can support improved decision-making in crop scheduling and management.

Keywords: *Zea mays* L.; phenology models; temperature; photoperiod

check for updates

Academic Editor: William A. Payne

Received: 20 August 2025
Revised: 19 September 2025
Accepted: 25 September 2025
Published: 26 September 2025

Citation: Liu, Y.-Y.; Su, Y.-C.; Sun, P.-W.; Dai, H.-Y.; Kuo, B.-J. Stability of Maize Phenology Predictions by Using Calendar Days, Thermal Functions, and Photothermal Functions. *Agriculture* **2025**, *15*, 2020. https://doi.org/10.3390/agriculture15192020

Copyright: © 2025 by the authors. Licensee MDPI, Basel, Switzerland. This article is an open access article distributed under the terms and conditions of the Creative Commons Attribution (CC BY) license (https://creativecommons.org/licenses/by/4.0/).

1. Introduction

Maize (*Zea mays* L.), an annual cereal of the Poaceae family originating from Central and South America, is one of the world's most important staple crops. By 2050, the global population is projected to reach 9 billion, and food demand is expected to increase by approximately 85%. Meeting anticipated demand for food will require current food production levels to be doubled [1,2]. How the yields of crops from limited arable land can be maximized is a critical challenge in the field of agriculture. To address potential food security, appropriate management strategies should be implemented at each stage of crop growth to enhance yields.

Crop phenology research focuses on the developmental stages and growth patterns of crops throughout the growing season and is critical for understanding crop dynamics and

optimizing agricultural management strategies [3,4]. In maize, flowering and maturity are two key stages. Flowering marks the onset of fertilization, during which female flowers receive pollen. Thereafter, kernels develop and accumulate nutrients until maturity, which signifies the completion of the maize growth cycle and readiness for harvest [5]. The physiological maturity corresponds to the maximum dry weight of kernels as well as the low grain moisture for better harvest quality [6,7]. Because environmental stresses during flowering can significantly affect maize yield, flowering is considered a critical phenological stage in crop modeling [8,9]. Therefore, these two stages hold substantial scientific value in maize phenology research, and understanding their characteristics is essential for improving crop management efficiency.

Crop development is influenced by environmental factors such as temperature [10], photoperiod [11], and water [12]. In maize, temperature and photoperiod are the two key factors in determining development. For temperature, the base temperature and optimum temperature are two critical temperatures for maize development. Maize has zero and maximum development rates at base temperature and optimum temperature, respectively [13]. 10 °C and 30 °C, as well as 8 °C and 34 °C, are two pairs of common base temperatures and optimum temperatures that are usually assumed for maize [10,14]. Regarding photoperiod, previous studies indicated that the tassel initiation of maize was delayed by increasing photoperiod [11,15,16]. The effect of photoperiod, namely, photoperiod sensitivity, was usually expressed as an increase in leaf number or extension of thermal duration per hour of photoperiod in excess of the critical photoperiod (12.5 h) [17]. However, different responses to photoperiod between maize varieties were reported [18]. Therefore, the development of maize is mainly determined by temperature and controlled by photoperiod, which depends on the genotype and day length of the location.

Predicting crop phenological stages accurately is essential for assessing crop development and guiding field management decisions such as fertilization and harvest timing [2,19]. Several indicators are used for representing the development progress of crops, including the number of days (days after sowing) and leaf number [9,20]. Growers often predict phenological stages on the basis of the number of days (calendar days) after crop sowing. This prediction method is relatively simple. However, because of the environmental factors' effects on crop development, the disadvantage of calendar days-based predictions is obvious under different growth conditions [14]. For instance, crops sown in high-temperature environments typically require fewer days to reach a given stage than do those sown in cooler environments; this leads to considerable variability in calendar day estimates. Consequently, applying this method to different cultivation regions may yield inconsistent outcomes, potentially resulting in suboptimal timings and unnecessary costs [21]. Additionally, Xu et al. [22] suggested that in maize, a longer photoperiod results in a greater duration of leaf initiation, leading to more leaves. Therefore, the inconsistent result of using leaf number as an indicator of maize development can be found when maize is cultivated in two distinct daylength conditions.

By the 18th century, researchers had recognized that for a crop to develop (i.e., reach flowering or maturity), it must have been exposed to a certain amount of heat. The total effective temperature accumulated during each of the crop phenological stages is called the accumulated temperature. Unlike the calendar days, the accumulated temperature for a given growth period tends to be constant regardless of location or year [23]. This understanding led to the introduction of the concept of accumulated heat units, which are now employed to predict crop phenological stages [10]. The relationship between temperature and maize development can be described using empirical or process-based approaches [24]. In crop models, various thermal functions are used to calculate accumulated temperature and simulate crop development, such as the CERES-Maize model [25] and the World Food

Studies (WOFOST) model [26]. These models differ in parameterization, data quality, and algorithmic complexity [24]. Therefore, the stabilities of these functions are expected to be different and need to be evaluated under current climate conditions. In addition, the stabilities of these functions are usually tested by evaluating the variation in the prediction of phenological stages [24] rather than the progress of maize development. Therefore, the stability of the prediction of maize dynamic development should be evaluated.

In addition to temperature, photoperiod regulates vegetative growth and flowering [27]. Unlike the temperature, the effect of photoperiod is included in part of maize crop models [28]. Most of these models use the concept of photoperiod sensitivity to predict the increase in leaf number or the extension of vegetative stage duration [17,18]. In addition, some researchers combined the effect of temperature and photoperiod through photothermal functions, such as the heliothermal unit (HTU), which incorporates sunshine duration, and the photothermal unit (PTU), which considers day length [29,30]. However, little is known about how the stability of photothermal functions depends on the underlying thermal functions from which they are derived, leaving a gap that this study aims to address.

This study's objective was to evaluate the stability of maize phenological stage predictions based on calendar days, thermal function (accumulated temperature), and photothermal function (accumulated HTUs or PTUs, hereafter collectively referred to as accumulated photothermal units). First, the stability of crop phenological predictions based on calendar days and various thermal functions was determined. Second, regression analysis was then employed to examine the relationship between the number of leaves and accumulated temperature to confirm the stability of the thermal-function-based predictions of leaf development progress. Finally, photothermal functions were incorporated into the predictions, and the stability of predictions made by considering calendar days, thermal function, and photothermal function was comprehensively determined to compare the performance between thermal function and photothermal function, as well as to evaluate the effect of thermal function on the stability of photothermal function.

2. Materials and Methods

2.1. Experimental Site and Design

Taiwan (22–25° N, 120–122° E), located at the intersection of the Eurasian continent and the Pacific Ocean, spans both tropical and subtropical monsoon climate zones. The experiment for this study was carried out in Taichung, Taiwan, at the Taiwan Agricultural Research Institute, Ministry of Agriculture (24.03° N, 120.69° E). The site has an average annual temperature of approximately 23.7 °C and average annual rainfall of 1762.8 mm. The soil at the site is classified as clay loam. Data on the following meteorological variables were collected during the experimental period: daily maximum temperature, daily minimum temperature, and daily sunshine hours (Figures A1 and A2). All meteorological data were obtained from the Agricultural Meteorological Observation Network monitoring system (https://agr.cwa.gov.tw/NAGR/history/station_day, accessed on 31 December 2024) or the Climate Data Inquiry Service (https://codis.cwa.gov.tw/StationData, accessed on 31 December 2024).

Maize experimental data were collected from 2021 to 2024. In 2021, a spring crop trial was conducted as a preliminary experiment using a randomized complete block design (RCBD) with four replications; the treatments consisted of different maize varieties. From the 2021 autumn maize season to the 2024 spring maize season, the experiments employed a split-plot design based on an RCBD framework. The main plot factor and subplot factor were sowing date and variety, respectively, and three replications were used. The blocks were arranged primarily according to the slope of the field. The varieties were randomly

planted in different plots. In central Taiwan, the recommended sowing period for maize is mid-February to mid-March for the spring crop season (S) and mid-to-late August for the fall crop season (F). The maize varieties used in the experiment, which had various maturity ratings, were Tainung No. 1 (TNG1), Tainung No. 7 (TNG7), and Ming-Feng No. 3. TNG1 and MF3 were selected because they are widely cultivated varieties in Taiwan, whereas TNG7 was included as a recently developed high-yielding and disease-resistant variety. All three varieties were grown across all cropping seasons and sowing dates throughout the study period. The average durations before flowering, after flowering, and for the whole growth period of these varieties under spring and fall conditions are summarized in Table 1. TNG1 has the shortest growth cycle (113.64–124.73 days), followed by TNG7 (119–135.57 days) and MF3 (123.2–139.2 days). For the spring crop season, the average durations of before flowering and after flowering are 67.27 days and 51.35 days, respectively. The fall crop season has a shorter duration before flowering than the duration after flowering. The experiments were conducted in Taichung, Taiwan, across seven crop seasons between 2021 and 2024. Detailed sowing dates for each crop season are listed in Table 2. The sowing dates range from mid-February to early April and late August to early October in the spring and fall crop seasons, respectively.

Table 1. Mean durations (number of days) and standard deviations before flowering of maize (from planting to anthesis), after its flowering (from flowering to maturity), and the whole growth period for three varieties. Values in the table are presented as mean (standard deviation).

Crop Season	Variety	Before Flowering	After Flowering	Whole Growth Period
Spring	TNG1	66.17 (5.12)	47.47 (3.56)	113.64 (6.49)
	TNG7	66.33 (4.87)	52.67 (4.53)	119.00 (7.17)
	MF3	69.30 (5.1)	53.90 (5.74)	123.20 (5.33)
	Mean	67.27	51.35	118.61
Fall	TNG1	55.17 (4.53)	69.57 (7.51)	124.73 (9.41)
	TNG7	57.20 (5.96)	78.37 (10.5)	135.57 (11.2)
	MF3	59.47 (5.06)	79.73 (9.27)	139.20 (10.2)
	Mean	57.28	75.89	133.17

Table 2. Field experiments conducted in Taichung, Taiwan, during 2021–2024.

Year	2021 Crop Season		2022 Crop Season		2023 Crop Season		2024 Crop Season
	Spring	Fall	Spring	Fall	Spring	Fall	Spring
Sowing date	February 23	August 31	March 3	August 23	February 15	September 19	February 16
		September 10	March 10	September 22	February 23	September 26	February 23
		September 27	March 17	September 27	March 8	October 3	April 10
			April 8	October 3	March 16	October 6	

Note: No maturity date was available for the 23 February 2021, 6 October 2023 and 10 April 2024 sowing date data.

2.2. Field Management and Data Collection

2.2.1. Field Management

Different crop seasons were coded to represent maize field data from various years (e.g., spring maize in 2021 was labeled as 2021-S). Experiment 2021-S was conducted in a 50 m × 10 m field, with plots of 6 m × 5 m and row and plant spacings of 0.75 m and 0.25 m, respectively, where seven rows were planted. All other experiments were carried out in 50 m × 50 m fields with plots of 8 m × 5 m and the same row and plant spacings; six rows were generally planted, except for experiment 2021-F, which had 10 rows. Two seeds were sown per hole, and seedlings were later thinned to one plant per hole at approximately 30 cm height. Fertilizer application included basal and top dressings. The basal fertilizer

(TFC#39 Biotec Organic Compound Fertilizer of Taiwan Fertilizer Company, Taiwan; 12-18-12-10 O.M.) was applied at 40 kg per 0.1 ha before sowing, and ammonium sulfate (40 kg per 0.1 ha) was top-dressed once around the six- to seven-leaf stages. Soil texture at the experimental site was classified as clay loam, with organic matter content and pH measured as described in Table A1. Irrigation was applied using the furrow irrigation method. The timing and frequency of irrigation events were determined according to field conditions and the prevailing weather in each cropping season, with an average of three to four applications per season. Pest and disease controls followed local agronomic practices, with insecticides such as spinetoram, novaluron, and flubendiamide, and herbicides such as glufosinate and atrazine, applied according to field conditions.

2.2.2. Field Measurements

Leaf Number Measurement: The number of fully expanded leaves on each plant was recorded by observing the appearance of leaf collars. For example, the date of emergence of the first visible leaf collar was counted as the appearance of the first leaf, the date of emergence of the second visible collar was counted as the second leaf, and so on. Leaf number was recorded for four central plants in each plot (three plants in experiment 2021-S), and markings were made using a permanent marker [9,31].

Flowering Stage Measurement: When the plants had reached the 12-leaf stage, preparations for observing the flowering stage began. Plots were observed three times per week, with an interval of 2 or 3 days between each observation. A plot was considered to have reached the flowering stage when 50% of the plants within it had flowered [24].

Physiological Maturity Measurement: This measurement was begun 40 days after flowering. Data were obtained three times per week, with intervals of 2 or 3 days between each observation. In each measurement, ears were randomly sampled from three plants. Physiological maturity was indicated by the disappearance of the milk line and formation of the black layer. The presence of black layers in 20 kernels from the middle section of each ear was the main criterion for maturity. If at least two of the three ears had more than 50% of kernels with visible black layers, the plot was considered to have reached physiological maturity [24].

2.3. Thermal Functions

Generally, the maize growth period can be divided into two phases: before flowering and after flowering. The phase before flowering refers to the period from planting to flowering, which is commonly known as the vegetative phenological stage. The phase after flowering covers the period from flowering to physiological maturity, representing the reproductive phenological stage. This study used recorded flowering and physiological maturity dates of maize varieties across different years and cropping seasons to calculate calendar days, accumulated temperature, and accumulated photothermal units from sowing to flowering and from flowering to maturity. These data were used to assess the stability of growth duration, thermal functions, and photothermal functions in predicting specific growth stages. For example, in 2021-S, variety TNG1 was sown on February 23 and flowered on May 1, with a growth duration of 67 days. Daily effective temperatures and photothermal units during this period were calculated and summed to obtain the accumulated values before flowering.

Crop models make use of several thermal functions to calculate accumulated temperature employing either an empirical or process-based approach [8]. Thermal functions can be applied within crop models to predict the timing of a crop's phenological stage and serve as a basis for developing cultivation plans. This study used the following eight thermal functions: growing degree days (GDD), specifically $GDD_{10,30}$ and $GDD_{8,34}$; thermal leaf

unit (TLU), enzymatic response (EnzymResp), Agricultural Production Systems Simulator (APSIM), crop heat unit (CHU), general thermal index (GTI), and WOFOST. Each function was used to calculate the daily development rate (DVR), which represents the daily effective temperature. The accumulated effective temperature over the maize growth period was obtained by summing the daily effective temperatures. The aforementioned thermal functions were adapted from those reported by Kumudini et al. [24] and Wang et al. [32].

The thermal functions used in this study can be classified into three main categories: empirical linear functions, empirical nonlinear functions, and process-based functions. Empirical functions are typically derived through statistical analysis of actual data and describe the relationships between variables. Such functions may be developed on the basis of field data. In this study, the empirical thermal functions used can be further categorized into linear and nonlinear functions. By contrast, process-based functions are developed on the basis of physical or physiological mechanisms and explicitly describe causal relationships between variables [33]. This study also includes functions based on protein activity. $GDD_{10,30}$ and $GDD_{8,34}$ are empirical linear functions. CHU and GTI are empirical nonlinear functions. TLU, APSIM, WOFOST, and EnzymResp are process-based functions. These thermal functions are described in the following.

1. Growing Degree Days ($GDD_{10,30}$)

The growing degree days (GDD) method is one of the simplest and most widely used approaches. $GDD_{10,30}$, based on the GDD model, is used to calculate the DVR as shown in Equation (1). In the model, the base temperature is 10 °C, and the optimum temperature is 30 °C, as described in Equations (2) and (3) [34].

$$\mathrm{DVR} = \mathrm{GDD}_{10,30} = \frac{(T_{max} + T_{min})}{2} - 10 \tag{1}$$

$$T_{max} = \begin{cases} 10\ ^{\circ}\mathrm{C}, & ObsT_{max} \leq 10\ ^{\circ}\mathrm{C} \\ ObsT_{max}, & 10\ ^{\circ}\mathrm{C} < ObsT_{max} < 30\ ^{\circ}\mathrm{C} \\ 30\ ^{\circ}\mathrm{C}, & ObsT_{max} \geq 30\ ^{\circ}\mathrm{C} \end{cases} \tag{2}$$

$$T_{min} = \begin{cases} 10\ ^{\circ}\mathrm{C}, & ObsT_{min} \leq 10\ ^{\circ}\mathrm{C} \\ ObsT_{min}, & 10\ ^{\circ}\mathrm{C} < ObsT_{min} < 30\ ^{\circ}\mathrm{C} \\ 30\ ^{\circ}\mathrm{C}, & ObsT_{min} \geq 30\ ^{\circ}\mathrm{C} \end{cases} \tag{3}$$

where $ObsT_{max}$ and $ObsT_{min}$ denote the observed daily maximum and minimum temperatures, respectively.

2. Growing Degree Days ($GDD_{8,34}$)

This calculation method is similar to that for $GDD_{10,30}$ except the GDD model sets T_{base} at 8 °C and the optimum temperature at 34 °C, which better reflects a suitable temperature range for maize growth [35]:

$$\mathrm{DVR} = \mathrm{GDD}_{8,34} = \sum_{i=1}^{24} (GDD_i/24) \tag{4}$$

$$GDD_i = T_i - 8 \tag{5}$$

In Equations (4) and (5), GDD_i is the function used to calculate the effective temperature for each hour, and T_i is the hourly temperature, which is estimated using a sine wave distribution during a 24 h period ([36]; Appendix A). The i subscript represents the i-th hour of the day, where i = 1, 2, …, 24. When T_i is less than 8 °C or more than 34 °C, its value is set to 8 °C and 34 °C, respectively.

3. General Thermal Index (GTI)

The GTI consists of two polynomial functions used to calculate maize's daily effective temperature. It is the only thermal function among those compared in this study that separates the calculations for the vegetative and reproductive growth stages. Equations (6) and (7) are used to calculate DVR during the vegetative and reproductive stages, respectively [37]:

$$\mathrm{DVR} = \mathrm{GTI_{veg}} = 0.043177 \times T_{mean}^2 - 0.000894 \times T_{mean}^3 \quad (6)$$

$$\mathrm{DVR} = \mathrm{GTI_{rep}} = 5.3581 + 0.011178 \times T_{mean}^2 \quad (7)$$

$$T_{mean} = (ObsT_{max} + ObsT_{min})/2 \quad (8)$$

where $\mathrm{GTI_{veg}}$ and $\mathrm{GTI_{rep}}$ represent the GTI values calculated for the vegetative and reproductive growth stages, respectively, and T_{mean} is the daily mean temperature, calculated as shown in Equation (8).

4. Crop Heat Unit (CHU)

The CHU calculation is shown in Equation (9). Different functions are applied for the day and night when calculating the daily effective temperature for maize. A quadratic function is used for the daytime, with minimum and optimum temperatures set at 10 and 30 °C, respectively [Equation (10)]. For nighttime, a linear function is applied, with a minimum temperature set at 4.4 °C [Equation (11); [38]]:

$$\mathrm{DVR} = [CHU(day) + CHU(night)]/2 \quad (9)$$

$$CHU(day) = 3.33 \times (ObsT_{max} - 10) - 0.084 \times (ObsT_{max} - 10)^2 \quad (10)$$

$$CHU(night) = 1.8 \times (ObsT_{min} - 4.4) \quad (11)$$

where *CHU*(*day*) and *CHU*(*night*) are the functions used to calculate the effective temperature during the day and night, respectively.

5. Thermal Leaf Unit (TLU)

DVR is calculated using TLU as expressed in Equation (12). TLU_{max} and TLU_{min} are calculated from T_{max} and T_{min}, respectively, and their averages are used to derive DVR, as shown in Equations (13) and (14). The minimum and maximum threshold temperatures for TLU are set at 6 and 44.8 °C, respectively, on the basis of the values employed in other maize studies [Equations (15) and (16); [24,36]].

$$\mathrm{DVR} = \mathrm{TLU} = \frac{TLU_{max} + TLU_{min}}{2} \quad (12)$$

$$TLU_{max} = 0.0997 - 0.036T_{max} + 0.00362{T_{max}}^2 - 0.0000639{T_{max}}^3 \quad (13)$$

$$TLU_{min} = 0.0997 - 0.036T_{min} + 0.00362{T_{min}}^2 - 0.0000639{T_{min}}^3 \quad (14)$$

$$T_{max} = \begin{cases} 6\ ^\circ\mathrm{C}, & ObsT_{max} \le 6\ ^\circ\mathrm{C} \\ ObsT_{max}, & 6\ ^\circ\mathrm{C} < ObsT_{max} < 44.8\ ^\circ\mathrm{C} \\ 44.8\ ^\circ\mathrm{C}, & ObsT_{max} \ge 44.8\ ^\circ\mathrm{C} \end{cases} \quad (15)$$

$$T_{min} = \begin{cases} 6\ ^\circ\mathrm{C}, & ObsT_{min} \le 6\ ^\circ\mathrm{C} \\ ObsT_{min}, & 6\ ^\circ\mathrm{C} < ObsT_{min} < 44.8\ ^\circ\mathrm{C} \\ 44.8\ ^\circ\mathrm{C}, & ObsT_{min} \ge 44.8\ ^\circ\mathrm{C} \end{cases} \quad (16)$$

where TLU_{max} and TLU_{min} represent TLU calculated using T_{max} and T_{min}, respectively.

6. Enzymatic Response (EnzymResp)

Johnson et al. [39] developed an equation to describe the temperature response of protein activity, and Parent and Tardieu [40] modified this equation to create a more intuitive version that is applicable to a wider temperature range. The EnzymResp equation is used to model the temperature response of protein activity. DVR is calculated with EnzymResp, as shown in Equation (17).

$$\mathrm{DVR} = \mathrm{EnzymResp} = \sum_{i=1}^{24}\left(\frac{EnzymResp_i}{24}\right) \tag{17}$$

$$EnzymResp_i = \frac{51559240052(T_i + 273)exp\left\{-\frac{73900}{[8.314(T_i+273)]}\right\}}{1 + exp\left(\frac{73900}{[8.314(T_i+273)]}\right)^{3.5\left(1-\frac{(T_i+273)}{306.4}\right)}} \tag{18}$$

In Equation (18), $EnzymResp_i$ is a function employed to calculate the effective temperature for each hour. T_i is the hourly temperature estimated using a sine wave distribution over a 24 h period [36]; The i subscript represents the i-th hour of the day, where $i = 1, 2, \ldots, 24$.

7. Agricultural Production Systems Simulator (APSIM)

Equation (19), based on the third-order polynomial model shown in Equation (20) [24], is employed to calculate DVR on the basis of APSIM. Minimum, optimum, and maximum temperatures are set at 0, 34, and 44 °C, respectively.

$$\mathrm{DVR} = \mathrm{APSIM} = \sum_{j=1}^{8} APSIM_j/8 \; j = 1, \ldots, 8 \tag{19}$$

$$APSIM_j = \begin{cases} 0, & T_j \le 0\ ^\circ\mathrm{C} \\ \frac{T_j}{1.8}, & 0\ ^\circ\mathrm{C} < T_j \le 18\ ^\circ\mathrm{C} \\ T_j - 8, & 18\ ^\circ\mathrm{C} < T_j \le 34\ ^\circ\mathrm{C} \\ 26 - \left[\left(T_j - 34\right) \times 2.6\right], & 34\ ^\circ\mathrm{C} < T_j \le 44\ ^\circ\mathrm{C} \\ 0, & T_j > 44\ ^\circ\mathrm{C} \end{cases} \tag{20}$$

where $APSIM_j$ is the function used to calculate the effective temperature every 3 h, and T_j is the temperature in each 3 h interval, estimated using a sine wave distribution over a 24 h period [36]; j represents the j-th 3 h interval of the day, where $j = 1, 2, \ldots, 8$.

8. World Food Studies (WOFOST)

In the WOFOST approach, DVR is calculated using daily thermal time as follows [26]:

$$\begin{aligned} \mathrm{DVR} &= \mathrm{WOFOST} \\ &= \begin{cases} 0, & ObsT_{mean} \le T_{base} \\ ObsT_{mean} - T_{base}, & T_{base} < ObsT_{mean} \le T_c \\ T_c - T_{base}, & ObsT_{mean} > T_c \end{cases} \end{aligned} \tag{21}$$

where $ObsT_{mean}$ denotes the observed daily mean temperature, and T_c is the upper temperature limit.

For a given thermal function, predicted maize DVR can vary under different temperature conditions, which suggests that the precision of a thermal function depends on the applied temperature range. To illustrate these differences, maize development rates were simulated under mean temperatures from 0 to 40 °C, assuming a diurnal temperature range

(DTR) of 10 °C, which approximates the average temperature observed in our dataset. The predicted DVRs were normalized for each function (Figure 1). The results highlighted distinct patterns among the categories of thermal functions. Empirical linear functions (e.g., GDD models) produced DVRs that increased proportionally with temperature. In contrast, empirical nonlinear functions and process-based functions showed curvilinear responses. Within the nonlinear functions, CHU and GTI_{veg} displayed similar curves, whereas GTI_{rep} showed a greater variation with temperature. The process-based functions produced a curvilinear response comparable to the empirical nonlinear functions. These differences, summarized in Figure 1, underscore the contrasting assumptions embedded in each thermal function and their implications for phenology prediction.

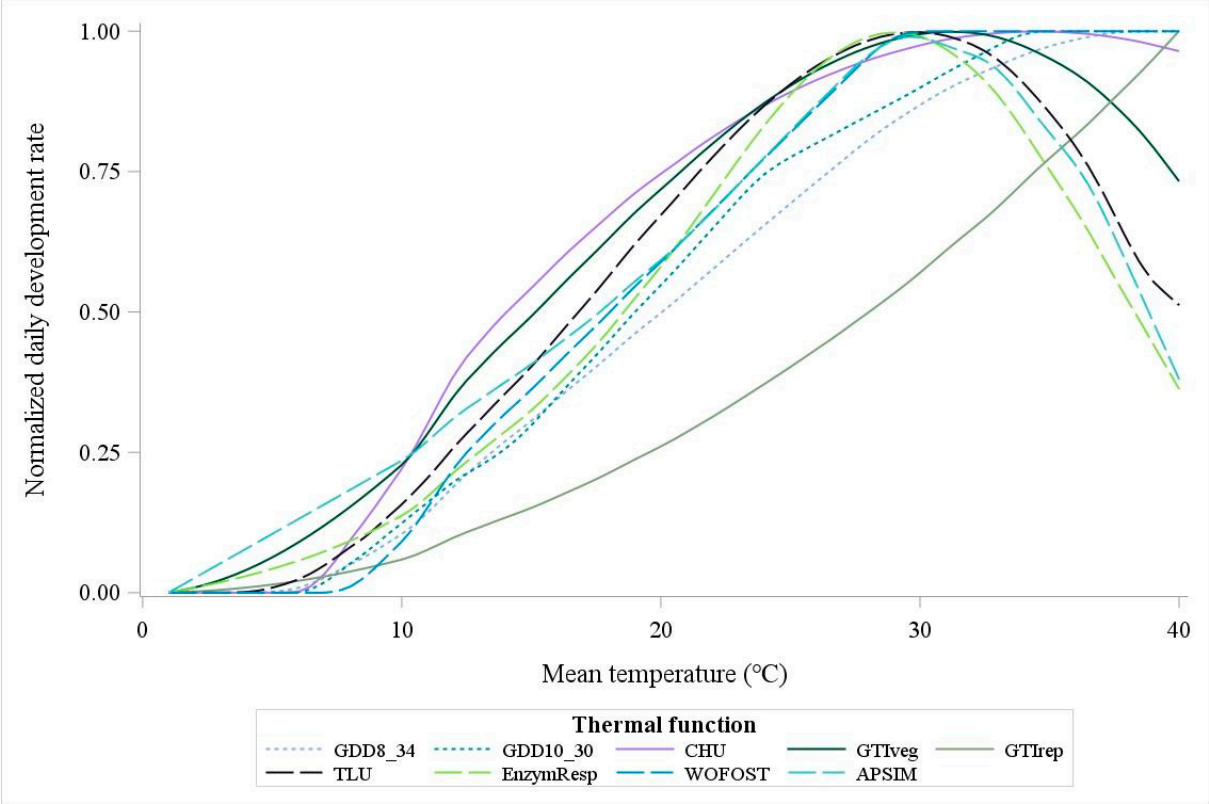


Figure 1. DVR versus mean daily temperature, obtained using the following thermal functions and mean daily temperatures with a 10 °C DTR.

2.4. Photothermal Functions

HTU and PTU incorporate both temperature and photoperiod to calculate accumulated photothermal units, expressed as follows [27,30,41]:

$$\mathrm{HTU} = \sum_{i=1}^{n} thermal \cdot SS \tag{22}$$

$$\mathrm{PTU} = \sum_{i=1}^{n} thermal \cdot DL \tag{23}$$

where n is the number of days from the sowing date to either the flowering stage or physiological maturity, *thermal* is the accumulated temperature calculated using a thermal function, *SS* is the actual sunshine hours, and *DL* refers to the maximum possible sunshine duration, also known as day length. In this study, the *SS* data were obtained from the national meteorological network. Both HTU and PTU were evaluated because they repre-

sent complementary ways of incorporating photoperiod effects: HTU accounts for actual sunshine duration, whereas PTU considers astronomical daylength.

2.5. Evaluation

The maize growth period was divided into two stages: before flowering and after flowering. For the spring crop, the sowing months were February, March, and April, and for the fall crop, the sowing months were August, September, and October. This study used calendar days, thermal functions, and photothermal functions to calculate the number of days, accumulated temperature, or accumulated photothermal units required for maize to reach specific phenological stages. The coefficient of variation (CV) was used to evaluate the stability of each method (calendar days vs. thermal functions vs. photothermal functions) for predicting maize phenological stages. The CV was calculated as follows:

$$\mathrm{CV} = \frac{s}{\overline{h}} \cdot 100 \tag{24}$$

where $\overline{h}$ and s represent the mean and standard deviation, respectively, of the values for calendar days, accumulated temperature, or accumulated photothermal units.

This study first evaluated the stability of calendar days and various thermal functions in calculating the number of days and accumulated temperature required for different maize varieties to reach specific phenological stages for crops with different sowing months. To this end, the CV for each variety was normalized by subtracting the minimum CV for that variety and dividing it by the full CV range. This normalization enabled a comparison of the differing sowing months. Next, the thermal function with the smallest CV was selected from each of the three categories (empirical linear, empirical nonlinear, and process-based functions). The selected thermal functions were then employed as part of the photothermal functions to calculate the accumulated temperature and accumulated photothermal units during maize growth. Finally, the stability of calendar days, thermal functions, and photothermal functions in predicting specific maize phenological stages was compared.

The relationship between leaf number and accumulated temperature was employed as an alternative approach to evaluate the stability of thermal functions [42]. Leaf number data from the hottest and coldest field seasons were fit to different thermal functions. A stable thermal function would result in similar accumulated temperature values required to reach a given leaf number, regardless of temperature variation during the growing period. The closeness of two regression lines was assessed using mean square error (MSE), root-mean-square error (RMSE), and mean absolute error (MAE). For each variety, these statistics were calculated using Equations (25)–(27).

$$\mathrm{MSE} = \frac{1}{n}\sum_{i=1}^{n}(x_i - y_i)^2 \tag{25}$$

$$\mathrm{RMSE} = \sqrt{\frac{1}{n}\sum_{i=1}^{n}(x_i - y_i)^2} \tag{26}$$

$$\mathrm{MAE} = \frac{1}{n}\sum_{i=1}^{n}|x_i - y_i| \tag{27}$$

where n is the total number of simulated values, x_i is the i-th simulated value from the first regression line, and y_i is the i-th simulated value from the second regression line. The nearer the MSE, RMSE, and MAE values to zero, the closer the two regression lines.

2.6. Data Analysis

All data analyses were performed using the SAS 9.4 statistical package (SAS Institute, Cary, NC, USA). The GLIMMIX procedure was employed to evaluate the stability of calendar days, thermal functions, and photothermal functions in predicting the specific phenological stages of maize. The generalized linear model assumed that the data followed a gamma distribution with a log link function. Analysis of variance (ANOVA) was first conducted to identify significant differences between group means. Multiple comparisons were performed only when significant differences were detected and were conducted using Hochberg's GT2 test.

3. Results and Discussion

3.1. Stability of Phenological Stage Predictions Obtained Using Calendar Days and Thermal Functions in Three Maize Varieties

This study used maize experimental data collected from 2021 to 2024 to evaluate the stability of phenological stage predictions, in terms of their CV value, for three varieties. Specifically, predictions based on calendar days were compared with those based on accumulated temperatures calculated using various thermal functions. Overall, thermal functions provided more stable predictions of maize phenological stages than the calendar days method, as reflected by consistently lower CVs across varieties and stages (Figure 2). The calendar days method produced the largest CVs, indicating lower stability, while GTI achieved the lowest average CV among all functions.

By variety, TNG7 showed the largest CVs in the before-flowering stage (6.85), whereas MF3 showed the largest CVs in the after-flowering stage (13.73). Varieties with longer growth durations (TNG7 and MF3) tended to have higher CVs than the early-maturing TNG1, suggesting that prediction stability may differ between short- and long-cycle varieties. Although Figure 2 does not allow direct statistical comparisons within each variety, the varietal patterns mirrored the overall averages. This reflects the differences among methods were consistent within the variety. In addition, when the thermal functions were classified into empirical linear, empirical nonlinear, and process-based functions, the average CVs for the before flowering stage were found to be ranked as follows: calendar days method > empirical nonlinear functions > process-based functions > empirical linear functions (Figure 2a). For the after-flowering stage, the ranking was calendar days method > empirical linear functions > process-based functions > empirical nonlinear functions (Figure 2b). Among thermal functions, APSIM performed best before flowering (5.70), whereas GTI was most stable after flowering (9.50). However, across both stages, GTI had the lowest overall average CV (7.74).

No matter what thermal functions were used, thermal functions had a better ability to predict maize development than the calendar days method [23,43,44]. These results indicate that the thermal functions well explained most of the maize development variations under different environments. A nonlinear relation between temperature and maize growth rate was reported in a previous study [43]. This relation corresponds to the relatively higher stability of empirical nonlinear thermal functions in our study and is also supported by a previous study [16]. Not only the nonlinear formations but also GTI's ability to separate vegetative and reproductive phases explain its superior performance. Zai et al. [45] observed superior performance of full growing season and reproductive stage predictions by GTI. Our result also indicates that the vegetative-stage formulation of GTI may still be refined. The findings of this study demonstrate that GTI is currently the most stable option under the experiment location's climatic conditions, which correspond to a subtropical climate. This indicates that temperature variations remain within a range where such functions are effective for predicting maize phenological stages.

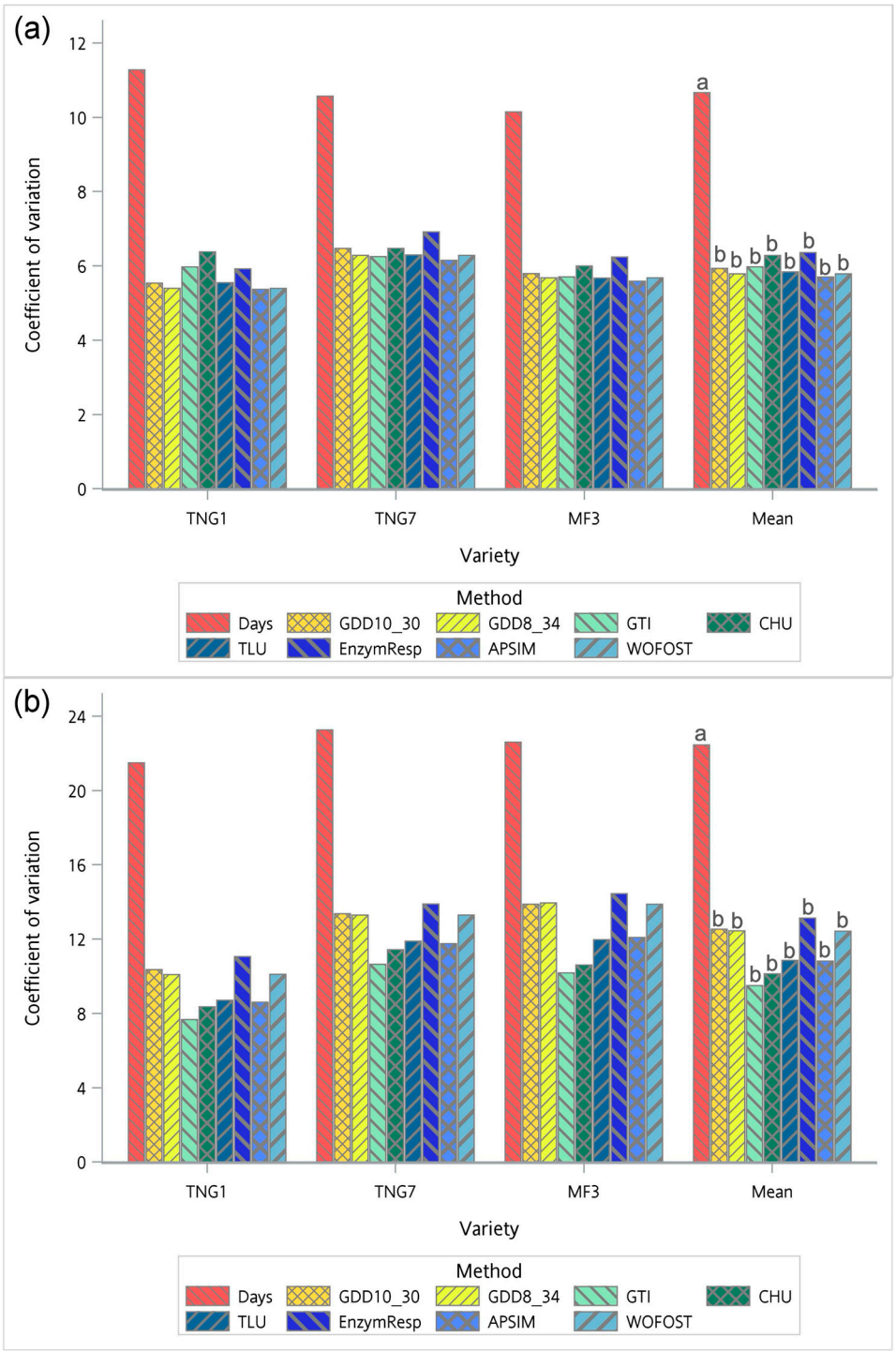


Figure 2. Bar charts showing the coefficients of variation of cumulative effective temperature during the growth period for each variety and method (Days, $GDD_{10,30}$, $GDD_{8,34}$, GTI, CHU, TLU, EnzymResp, APSIM, and WOFOST): (**a**) before flowering stage (from planting to flowering), with a total sample size of 73 per variety; and (**b**) after flowering stage (from flowering to maturity), with a total sample size of 60 per variety. Means followed by different letters indicate significant differences at the 0.05 probability level, as determined using Hochberg's GT2 test.

3.2. Stability of Phenological Stage Predictions Obtained Using Calendar Days and Thermal Functions for Various Sowing Dates

This study also evaluated the stability of the phenological stage predictions of thermal functions between different sowing months. The calendar days method was used to calculate the number of days, and the accumulated temperature was calculated using the

thermal functions. The CV for each method given the sowing months was then computed to determine the stability of the predictions. Overall, predictions for maize sown in March (spring crop season) and September (fall crop season) were less stable than those for other sowing months, regardless of the method used (Table 3). Across most sowing months, thermal functions produced lower CVs than the calendar days method, confirming their superior stability. In the before- and after-flowering stages, CVs were consistently larger for maize sown in March and September than for maize sown in other months of the crop season. These results indicate that the instability in predicting maize phenological stages when using accumulated temperature from various thermal functions primarily occurs in the data associated with sowing in March and September.

Table 3. Coefficient of variation (CV) for the before-flowering stage (from planting to flowering) and the after-flowering stage (from flowering to maturity), calculated using the number of growing days and the accumulated temperature determined using various thermal functions. The data include all maize varieties with different sowing dates from February to October between 2021 and 2024. The total number of observations is 42 for the before-flowering stage and 33 for the after-flowering stage.

		Coefficient of Variation (%)									
	Sowing Date	**Days**	**$GDD_{10,30}$**	**$GDD_{8,34}$**	**GTI**	**CHU**	**TLU**	**EnzymRes**	**APSIM**	**WOFOST**	**Mean**
Before flowering	Spring										
	February	2.57 ns	2.86 ns	2.80 ns	2.58 ns	2.52 ns	2.76 ns	2.87 ns	2.71 ns	2.80 ns	2.72
	March	3.22 ns	3.71 ns	3.63 ns	3.37 ns	3.45 ns	3.67 ns	3.76 ns	3.56 ns	3.63 ns	3.55
	April	2.01 ns	2.18 ns	2.20 ns	2.09 ns	2.13 ns	2.16 ns	2.20 ns	2.20 ns	2.20 ns	2.15
	Fall										
	August	2.50 ab	2.08 ab	1.98 ab	2.18 ab	2.21 ab	2.11 ab	2.01 ab	1.99 ab	1.99 ab	2.12
	September	5.38 a	3.53 a	3.63 a	3.81 a	3.86 a	3.59 a	3.56 a	3.67 a	3.63 a	3.85
	October	1.84 b	1.53 b	1.54 b	1.62 b	1.64 b	1.55 b	1.50 b	1.55 b	1.54 b	1.59
After flowering	Spring										
	February	3.65 ns	3.42 ns	3.49 ns	3.44 ns	3.43 ns	3.41 ns	3.41 ns	3.47 ns	3.48 ns	3.47
	March	4.53 ns	3.90 ns	3.96 ns	3.89 ns	4.03 ns	3.92 ns	3.85 ns	3.95 ns	3.96 ns	4.00
	April	2.10 ns	2.04 ns	2.03 ns	1.94 ns	2.09 ns	2.06 ns	2.03 ns	2.02 ns	2.01 ns	2.04
	Fall										
	August	1.71 b	1.94 ns	1.91 ns	1.73 b	1.80 ns	1.90 ns	1.96 ns	1.86 ns	1.91 ns	1.86
	September	6.43 a	4.59 ns	4.58 ns	5.03 a	4.93 ns	4.55 ns	4.67 ns	4.71 ns	4.58 ns	4.90
	October	2.68 ab	2.66 ns	2.72 ns	2.62 ab	2.69 ns	2.67 ns	2.67 ns	2.69 ns	2.72 ns	2.68

Note: A multiple comparison analysis was conducted separately for the spring and fall seasons within a column. ns indicates a lack of statistical significance, as determined using ANOVA, and means followed by different letters indicate statistically significant differences between sowing dates at the 0.05 probability level, as determined using Hochberg's GT2 test.

The stability of the thermal-function-based predictions was related to the functions' responses over a wider temperature range [24]. These results may have been influenced by DTR, defined as the difference between daily maximum and minimum temperatures. Regarding the before-flowering stage, the maximum DTRs for spring maize sown in February, March, and April were 23.9, 25.6, and 19.0 °C, respectively (Figure A1). For fall maize sown in August, September, and October, the maximum DTRs were 19.1, 24.3, and 23.2 °C. In the after-flowering stage, the maximum DTRs for February, March, and April sowings were 17.6, 19.1, and 13.6 °C, whereas those for August, September, and October sowings were 16.1, 28.4, and 28.6 °C. Except for the after-flowering period of fall maize, the largest DTR values were consistently found in March and September, which

were also the months with the highest CVs. Maximum DTR values were consistently observed during the growth periods of maize sown in March and September, coinciding with the months that showed the greatest prediction instability. This indicates that thermal functions are highly sensitive to temperature fluctuations and that sowing time strongly modulates prediction stability. It is important to note that these findings are specific to the location of the experiments, where maximum daily temperatures during the trials did not exceed 37 °C. Validation with data from other regions and wider thermal ranges is needed to assess the robustness of these functions. Wang et al. [32] compared six models for estimating maize DVR. The results showed that once the temperature exceeded the optimal range for maize, the DVRs varied significantly. Their study also indicated that, in future climate scenarios, the uncertainty in simulating maize phenology will increase as temperature increases beyond the optimal range. In crop models, the optimal and maximum temperatures are key parameters for estimating a crop's DVR. However, if the parameters estimated under higher-temperature conditions still exhibit a considerable uncertainty, this situation would negatively affect the reliability [42]. Therefore, future research could further explore the response of thermal functions in predicting a crop's DVR when temperatures exceed the optimal range. This could improve the predictive ability of thermal functions beyond the optimal temperature and reduce uncertainty, ultimately enhancing such functions' application in crop models to improve these models' ability to simulate phenological stages.

The calendar days method occasionally produced lower CVs than thermal functions in spring maize, likely because weather conditions of different sowing dates were relatively uniform within the same sowing month. This suggests that calendar days may be useful in regions with stable climates but are less reliable when used across multiple locations [21]. A relatively high CV of the predictions of thermal functions across locations was also found and explained by the other factors, such as water and nutrients [23]. This indicates a need to incorporate other factors in the prediction of phenological stages.

3.3. Evaluating Thermal Function Stability by Using the Cumulative Temperature and Leaf Number Relationship

Of the empirical linear, empirical nonlinear, and process-based thermal functions, $GDD_{8,34}$, GTI, and APSIM, respectively, were identified in the CV evaluation as being the most stable for predicting maize phenological stage (Figure 2). Subsequently, thermal functions were used to fit the leaf number during the vegetative growth period of maize under the warmest and coldest climatic conditions observed in the trials. The irrigation and fertilizers were applied to ensure an unlimited supply of water and nutrition for maize. This analysis assumed that the development of the leaf was solely influenced by temperature and was conducted to determine the stability of each thermal function in predicting the phenological stages of maize. Suppose a thermal function can consistently predict the accumulated temperature required to reach a specific leaf number. This would imply that for a given leaf number, the accumulated temperature is the same regardless of the climatic temperature during the growing period.

Overall, GTI showed the greatest stability in capturing the relationship between accumulated temperature and maize leaf development, outperforming $GDD_{8,34}$ and APSIM across varieties (Figure 3). Regression analyses under the warmest and coldest growing conditions revealed that GTI consistently produced smaller deviations between temperature scenarios, as reflected by lower MSE (0–0.06), RMSE (0.05–0.24), and MAE (0.04–0.21) values, leading to the following ranking of stability: GTI > $GDD_{8,34}$ > APSIM. Compared to the cold condition, $GDD_{8,34}$ and APSIM underestimated the leaf number in the hot condition. In other words, these two functions overestimated the accumulated temperature in the hot condition. Furthermore, the range of the x-axis indicated that $GDD_{8,34}$ and

APSIM perform a higher accumulated temperature than GTI. For TNG1, the regression lines derived from GTI were closer than those obtained from $GDD_{8,34}$ and APSIM. Similar results were observed for TNG7 and MF3. Therefore, the results were consistent between varieties.

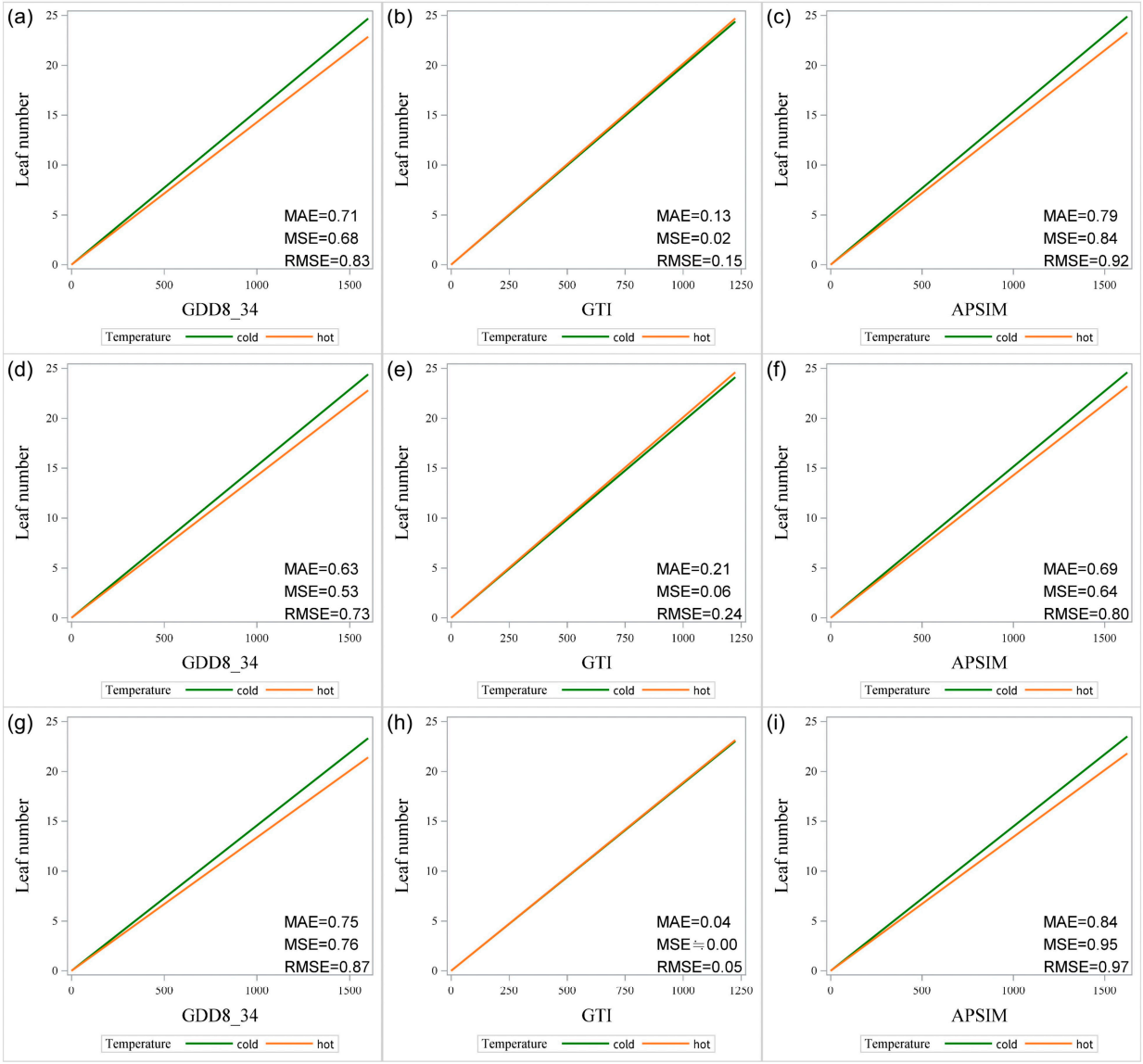


Figure 3. Relationship between leaf number and cumulative temperature for each variety, where predictions were obtained using (**a**) $GDD_{8,34}$, (**b**) GTI, and (**c**) APSIM for TNG1; (**d**) $GDD_{8,34}$, (**e**) GTI, and (**f**) APSIM for TNG7; (**g**) $GDD_{8,34}$, (**h**) GTI, and (**i**) APSIM for MF3. The orange and green lines represent data from the before flowering stage (from planting to flowering) under high temperature and the growing season under low temperature, respectively. MSE, RMSE, and MAE values indicating performance of leaf number predictions obtained using three thermal functions ($GDD_{8,34}$, GTI, and APSIM) for three varieties when considering planting to flowering phenological stages.

This analysis was conducted under uniform irrigation and nutrient management across all trials, thereby minimizing potential variability from water or fertilizer differences. Nevertheless, the effects of soil moisture and nutrient status on maize leaf development were not explicitly analyzed. This represents a limitation of the present study, as these factors are also known to influence leaf initiation and expansion [46]. Future studies should incorporate such variables to more comprehensively evaluate the phenological stability.

3.4. Stability of Phenological Stage Predictions Obtained Using Calendar Days, Thermal Functions, and Photothermal Functions

In this study, the $GDD_{8,34}$, GTI, and APSIM thermal functions were further integrated with photoperiod variables to construct photothermal functions. The CVs of phenological stage predictions were compared between calendar days, accumulated temperature, and accumulated photothermal unit methods to quantify the stability of predictions. The results were expected to clarify whether photothermal function can provide a more stable prediction of phenological stage, and the importance of selecting a stable thermal function to construct the photothermal function.

Overall, thermal functions provided the most stable predictions, consistently outperforming both the calendar days and photothermal functions (Figure 4). By contrast, photothermal functions (PTU and HTU) were generally the least stable and often yielded larger CVs than the calendar days method. Across varieties and stages, CVs derived from thermal functions were consistently lower than those from photothermal functions and calendar days. Although the direct statistical comparisons within each variety were not allowed, the varietal patterns mirrored the overall averages. This reflects the differences among methods were consistent within the variety. In terms of varieties, TNG7 had the highest CV (11.59) in the before-flowering stage, whereas MF3 had the highest CV (22.17) in the after-flowering stage. Despite these varietal differences, the overall ranking of stability was clear: thermal functions > calendar days > photothermal functions. Within photothermal functions, HTU consistently produced the largest CVs among the methods, indicating that predictions using HTU were the most unstable. Specifically, HTU_{GDD}, HTU_{GTI}, and HTU_{APSIM} yielded significantly larger CVs than other methods, confirming that HTU was less stable. Within the PTU photothermal function, PTU_{GTI} performed a lower CV in all varieties and had a significantly lower average CV than PTU_{GDD} and PTU_{APSIM} in the after-flowering stage. This indicates that the stability of the photothermal function is affected by the thermal function. Therefore, selecting a stable thermal function is important for constructing a stable photothermal function.

Three factors (physiology, environment, and functional structure) were used to explain the poor results of the photothermal functions. Physiological factors indicated the photoperiod sensitivity of the varieties in our study. The photoperiod sensitivity was found to vary between maize genotypes [18]. The maize varieties used in this study are relatively insensitive to photoperiod. In addition, because of the low latitude of Taiwan, day length rarely exceeded 12.5 h during the maize growing seasons, especially in spring. Therefore, the effect of photoperiod on maize development was limited. Furthermore, the critical photoperiod (12.5 h) is not incorporated into the HTU or PTU functions. This probably over-weighted the effect of photoperiod on maize development. According to the study of Kiniry et al. [11], maize is only sensitive to photoperiod during the inductive stage (end of juvenile to tassel initiation). Therefore, using photoperiod variables of a full growing season in the photothermal functions is improper and also overly weights the effect of photoperiod on maize development. In addition, crop models usually use day length rather than sunshine hours to incorporate the effect of photoperiod into maize development prediction [17,18]. Therefore, the poorest performance of HTU can be explained by its calculation mechanism: when sunshine hours are zero, HTU records no accumulation, even though heat still accumulates. This structural limitation leads to instability, particularly under cloudy conditions. By contrast, thermal functions that rely solely on temperature avoid this issue, explaining their greater stability. Under such conditions, temperature dominates development, making photothermal functions less effective. Previous studies also report that accumulated temperature is more reliable for maize phenology prediction than sunshine-based metrics [47,48]. Thus, the stronger stability of thermal functions is

consistent with physiological expectations for maize grown in Taiwan. However, it should be noted that this study focused on environments with a limited variation in day length and did not explicitly test conditions where photoperiod-sensitive varieties or higher latitudes may enhance the relevance of photothermal functions. Future research should evaluate whether photothermal metrics provide a greater explanatory power under such conditions.

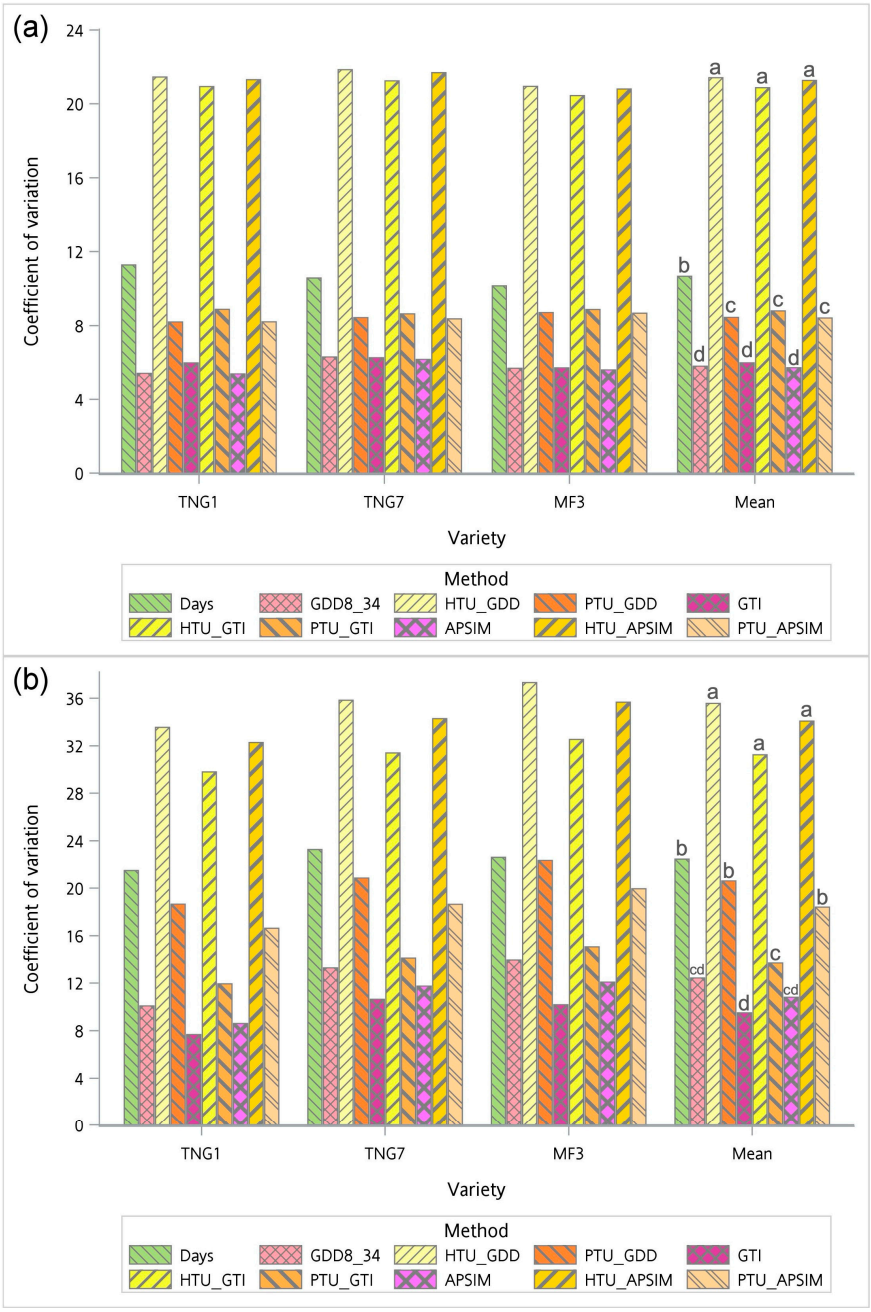


Figure 4. Bar charts showing the coefficients of variation (CV) for the number of days, accumulated temperature, and accumulated photothermal units during the growth period, for different varieties and methods: calendar days (Days), thermal functions ($GDD_{8,34}$, GTI, APSIM), and photothermal functions (HTU and PTU): (**a**) before flowering stage (from planting to flowering), with a total sample size of 73 per variety; and (**b**) after flowering stage (from flowering to maturity), with a total sample size of 60 per variety. Means followed by different letters indicate significant differences at the 0.05 probability level, as determined using Hochberg's GT2 test.

4. Conclusions

This study demonstrated that thermal functions provide more stable predictions of maize phenology than the calendar days and photothermal methods. Among thermal functions, the empirical nonlinear function GTI proved to be the most stable under the experiment's climatic conditions. By contrast, photothermal functions, especially HTU, were less reliable, often performing worse than the calendar days method. These results highlight the importance of selecting appropriate thermal functions, particularly GTI, to improve the accuracy and stability of phenological predictions.

Author Contributions: Data curation, Y.-Y.L. and Y.-C.S.; Formal analysis, Y.-Y.L.; Funding acquisition, B.-J.K.; Investigation, Y.-Y.L. and Y.-C.S.; Methodology, Y.-Y.L. and Y.-C.S.; Resources, P.-W.S. and H.-Y.D.; Supervision, B.-J.K.; Writing—original draft, Y.-Y.L. and Y.-C.S.; Writing—review and editing, B.-J.K. All authors have read and agreed to the published version of the manuscript.

Funding: This manuscript was professionally edited by Wallace Academic Editing. This research was supported (in part) by the projects NSTC 111-2634-F-005-001, NSTC 112-2634-F-005-002, and NSTC 113-2634-F-005-002 of the Smart Sustainable New Agriculture Research Center (SMARTer), as well as by project MOST 110-2313-B-005-010-MY3.

Data Availability Statement: The original contributions presented in this study are included in the article. Further inquiries can be directed to the corresponding author(s).

Conflicts of Interest: The authors declare no conflicts of interest.

Abbreviations

The following abbreviations are used in this manuscript:

APSIM	agricultural production systems simulator
ANOVA	analysis of variance
CHU	crop heat units
CV	coefficient of variation
Days	calendar days
DTR	diurnal temperature range
DVR	daily development rate
EnzymResp	enzymatic response
GDD	growing degree days
GTI	general thermal index
GTI_{rep}	general thermal index during the reproductive growth period
GTI_{veg}	general thermal index during the vegetative growth period
HTU	heliothermal units
HTU_{APSIM}	heliothermal units with APSIM
HTU_{GDD}	heliothermal units with $GDD_{8,34}$
HTU_{GTI}	heliothermal units with GTI
MAE	mean absolute error
MSE	mean square error
PTU	photothermal units
PTU_{APSIM}	photothermal units with APSIM
PTU_{GDD}	photothermal units with $GDD_{8,34}$
PTU_{GTI}	photothermal units with GTI
RCBD	randomized complete block design
RMSE	root-mean-square error
TLU	thermal leaf units
WOFOST	World Food Studies

Appendix A

Regarding the calculation of temperature by using a sine wave [16], an example is provided for calculating the temperature on an hourly basis:

$$T_i = \frac{T_{max} + T_{min}}{2} + \frac{T_{max} - T_{min}}{2} \cos\left[\frac{(i-1)\pi}{12}\right]$$

where T_i represents the temperature in the i-th hour of the day, where $i = 1, 2, \ldots, 24$; T_{max} is the daily maximum temperature; and T_{min} is the daily minimum temperature.

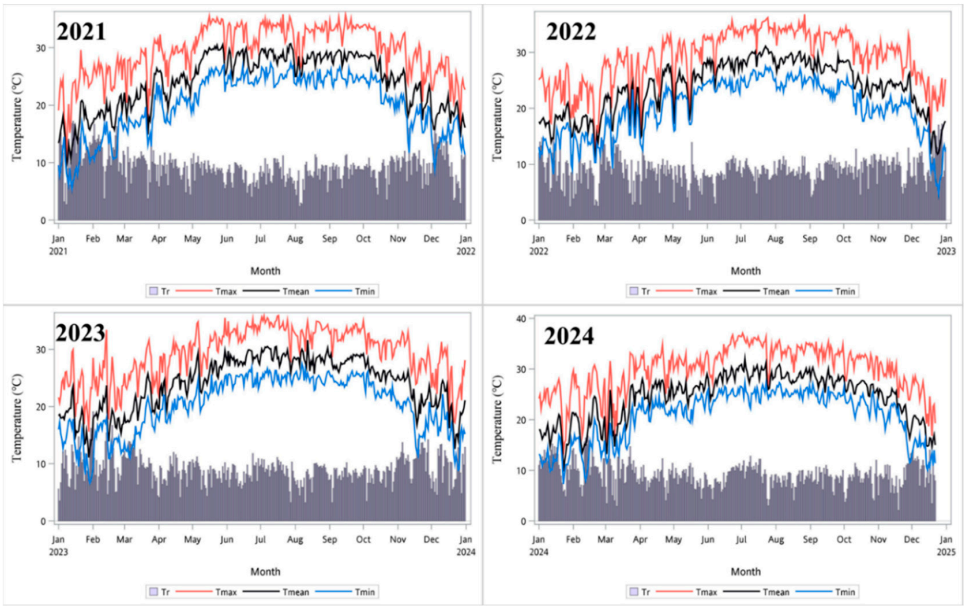


Figure A1. Daily maximum temperature (T_{max}), mean temperature (T_{mean}), and minimum temperature (T_{min}) and diurnal temperature range (T_r) during 2021–2024 crop seasons.

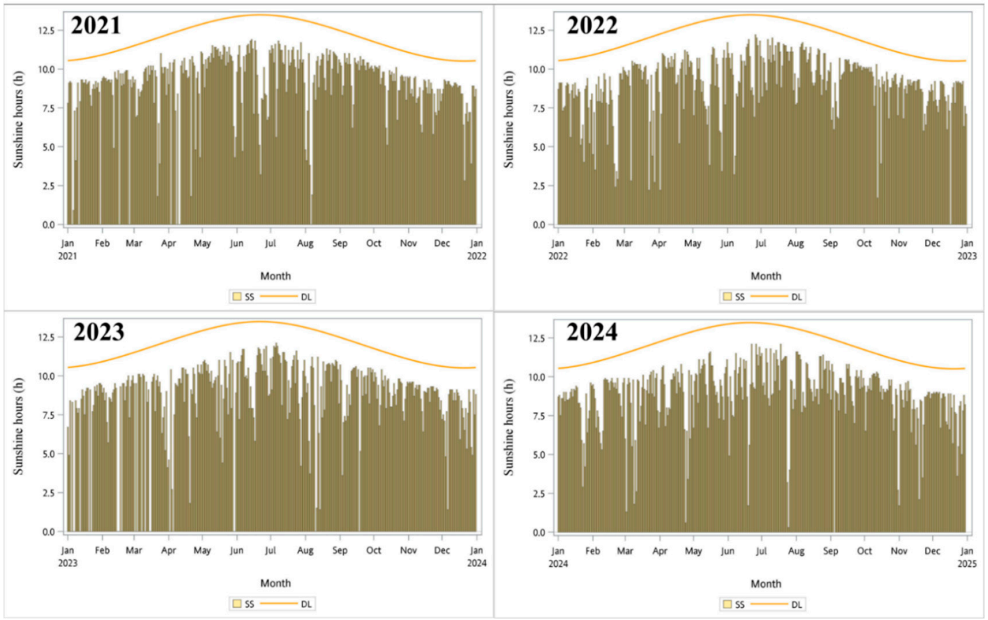


Figure A2. Daily actual solar hours (*SS*) and maximum possible sunshine hours (*DL*) during 2021–2024 crop seasons.

Table A1. Soil properties of the experimental site.

Experiment Code	Soil Texture	Organic Matter (%)	pH
2021-S	clay loam	2.14	5.86
2021-F	clay loam	2.21	6.28
2022-S	clay loam	1.83	6.03
2022-F	clay loam	1.64	5.89
2023-S	clay loam	2.07	5.61
2023-F	clay loam	1.15	6.59
2024-S	clay loam	2.24	5.59

Note: Organic matter content was determined following the method of Nelson and Sommers [49]. Soil pH was measured according to the NIEA S410.62C protocol, with 20 mL of reagent water added.

References

1. Raza, A.; Razzaq, A.; Mehmood, S.S.; Zou, X.; Zhang, X.; Lv, Y.; Xu, J. Impact of climate change on crops adaptation and strategies to tackle its outcome: A review. *Plants* **2019**, *8*, 34. [CrossRef]
2. Janni, M.; Maestri, E.; Gulli, M.; Marmiroli, M.; Marmiroli, N. Plant responses to climate change, how global warming may impact on food security: A critical review. *Front. Plant Sci.* **2024**, *14*, 1297569. [CrossRef] [PubMed]
3. Luo, Y.-C.; Zhang, Z.; Zhang, L.-L.; Zhang, J.; Tao, F.-L. Weakened maize phenological response to climate warming in China over 1981–2018 due to cultivar shifts. *Adv. Clim. Change Res.* **2022**, *13*, 710–720. [CrossRef]
4. Qin, M.; Li, R.; Ye, H.; Nie, C.; Zhang, Y. Study on the Extraction of Maize Phenological Stages Based on Multiple Spectral Index Time-Series Curves. *Agriculture* **2024**, *14*, 2052. [CrossRef]
5. Wu, H.; Liu, B.; Zhu, B.; Zhen, Z.; Song, K.; Ren, J. Combining Vegetation Indices to Identify the Maize Phenological Information Based on the Shape Model. *Agriculture* **2024**, *14*, 1608. [CrossRef]
6. Sala, R.G.; Andrade, F.H.; Westgate, M.E. Maize kernel moisture at physiological maturity as affected by the source–sink relationship during grain filling. *Crop Sci.* **2007**, *47*, 711–714. [CrossRef]
7. Gao, S.; Ming, B.; Li, L.-l.; Yin, X.-b.; Xue, J.; Wang, K.-r.; Xie, R.-z.; Li, S.-k. Relationship and distribution of in-field dry-down and equilibrium in maize grain moisture content. *Agric. For. Meteorol.* **2021**, *304*, 108409. [CrossRef]
8. Wang, Y.; Tao, H.; Tian, B.; Sheng, D.; Xu, C.; Zhou, H.; Huang, S.; Wang, P. Flowering dynamics, pollen, and pistil contribution to grain yield in response to high temperature during maize flowering. *Environ. Exp. Bot.* **2019**, *158*, 80–88. [CrossRef]
9. dos Santos, C.L.; Abendroth, L.J.; Coulter, J.A.; Nafziger, E.D.; Suyker, A.; Yu, J.; Schnable, P.S.; Archontoulis, S.V. Maize leaf appearance rates: A synthesis from the United States Corn Belt. *Front. Plant Sci.* **2022**, *13*, 872738. [CrossRef]
10. Ritchie, J.T.; Nesmith, D.S. Temperature and crop development. In *Modeling Plant and Soil Systems*; Hanks, J., Ritchie, J.T., Eds.; Agronomy Monograph 31; ASA, CSSA, SSSA: Madison, WI, USA, 1991; pp. 5–29. [CrossRef]
11. Kiniry, J.; Ritchie, J.; Musser, R. Dynamic Nature of the Photoperiod Response in Maize 1. *Agron. J.* **1983**, *75*, 700–703. [CrossRef]
12. Wopereis, M.; Kropff, M.; Maligaya, A.; Tuong, T. Drought-stress responses of two lowland rice cultivars to soil water status. *Field Crops Res.* **1996**, *46*, 21–39. [CrossRef]
13. Tsimba, R.; Edmeades, G.O.; Millner, J.P.; Kemp, P.D. The effect of planting date on maize: Phenology, thermal time durations and growth rates in a cool temperate climate. *Field Crops Res.* **2013**, *150*, 145–155. [CrossRef]
14. Cross, H.; Zuber, M. Prediction of flowering dates in maize based on different methods of estimating thermal units 1. *Agron. J.* **1972**, *64*, 351–355. [CrossRef]
15. Warrington, I.; Kanemasu, E. Corn Growth Response to Temperature and Photoperiod. III. Leaf Number 1. *Agron. J.* **1983**, *75*, 762–766. [CrossRef]
16. Ellis, R.; Summerfield, R.; Edmeades, G.; Roberts, E. Photoperiod, temperature, and the interval from sowing to tassel initiation in diverse cultivars of maize. *Crop Sci.* **1992**, *32*, 1225–1232. [CrossRef]
17. Birch, C.; Hammer, G.L.; Rickert, K. Temperature and photoperiod sensitivity of development in five cultivars of maize (*Zea mays* L.) from emergence to tassel initiation. *Field Crops Res.* **1998**, *55*, 93–107. [CrossRef]
18. Hunter, R.; Hunt, L.; Kannenberg, L. Photoperiod and temperature effects on corn. *Can. J. Plant Sci.* **1974**, *54*, 71–78. [CrossRef]
19. Potgieter, A.B.; Zhao, Y.; Zarco-Tejada, P.J.; Chenu, K.; Zhang, Y.; Porker, K.; Biddulph, B.; Dang, Y.P.; Neale, T.; Roosta, F.; et al. Evolution and application of digital technologies to predict crop type and crop phenology in agriculture. *In Silico Plants* **2021**, *3*, diab017. [CrossRef]
20. Zhao, Y.; Meng, Y.; Han, S.; Feng, H.; Yang, G.; Li, Z. Should phenological information be applied to predict agronomic traits across growth stages of winter wheat? *Crop J.* **2022**, *10*, 1346–1352. [CrossRef]

21. Liu, Y.; Xie, R.; Hou, P.; Li, S.; Zhang, H.; Ming, B.; Long, H.; Liang, S. Phenological responses of maize to changes in environment when grown at different latitudes in China. *Field Crops Res.* **2013**, *144*, 192–199. [CrossRef]
22. Xu, H.; Ming, B.; Wang, K.; Xue, J.; Hou, P.; Li, S.; Xie, R. The effects of photoperiod and temperature-related factors on maize leaf number and leaf positional distribution in the field. *Front. Plant Sci.* **2023**, *14*, 1006245. [CrossRef]
23. Soler, C.T.; Sentelhas, P.; Hoogenboom, G. Thermal time for phenological development of four maize hybrids grown off-season in a subtropical environment. *J. Agric. Sci.* **2005**, *143*, 169–182. [CrossRef]
24. Kumudini, S.; Andrade, F.H.; Boote, K.J.; Brown, G.A.; Dzotsi, K.A.; Edmeades, G.O.; Gocken, T.; Goodwin, M.; Halter, A.L.; Hammer, G.L.; et al. Predicting maize phenology: Intercomparison of functions for developmental response to temperature. *Agron. J.* **2014**, *106*, 2087–2097. [CrossRef]
25. Jones, J.W.; Hoogenboom, G.; Porter, C.H.; Boote, K.J.; Batchelor, W.D.; Hunt, L.; Wilkens, P.W.; Singh, U.; Gijsman, A.J.; Ritchie, J.T. The DSSAT cropping system model. *Eur. J. Agron.* **2003**, *18*, 235–265. [CrossRef]
26. De Wit, A.; Boogaard, H.; Supit, I.; van den Berg, M. *System Description of the WOFOST 7.2 Cropping Systems Model*; Wageningen Environmental Research: Wageningen, The Netherlands, 2020.
27. Liao, Z.-q.; Zheng, J.; Fan, J.-l.; Pei, S.-z.; Dai, Y.-l.; Zhang, F.-c.; Li, Z.-j. Novel models for simulating maize growth based on thermal time and photothermal units: Applications under various mulching practices. *J. Integr. Agric.* **2023**, *22*, 1381–1395. [CrossRef]
28. Bassu, S.; Brisson, N.; Durand, J.L.; Boote, K.; Lizaso, J.; Jones, J.W.; Rosenzweig, C.; Ruane, A.C.; Adam, M.; Baron, C. How do various maize crop models vary in their responses to climate change factors? *Glob. Change Biol.* **2014**, *20*, 2301–2320. [CrossRef]
29. Nuttonson, M.Y. Some preliminary observations of phenological data as a tool in the study of photoperiodic and thermal requirements of various plant material. In *Vernalization and Photoperiodism*; Murneek, A.E., Whyte, R.O., Eds.; Chronica Botanica: Waltham, MA, USA, 1948; pp. 129–143. Available online: https://www.cabidigitallibrary.org/doi/full/10.5555/19490701172 (accessed on 4 March 2025).
30. Robertson, G.W. A biometeorological time scale for a cereal crop involving day and night temperatures and photoperiod. *Int. J. Biometeorol.* **1968**, *12*, 191–223. [CrossRef]
31. Bell, J. *Corn Growth Stages and Development*; Texas A&M University: College Station, TX, USA, 2024.
32. Wang, N.; Wang, J.; Wang, E.; Yu, Q.; Shi, Y.; He, D. Increased uncertainty in simulated maize phenology with more frequent supra-optimal temperature under climate warming. *Eur. J. Agron.* **2015**, *71*, 19–33. [CrossRef]
33. Lu, H.Y. The meanings and outlook of crop modeling. *Taiwan Agric. Bimon.* **1997**, *33*, 12–20.
34. Gilmore, E.C.; Rogers, J.S. Heat units as a method of measuring maturity in corn. *Agron. J.* **1958**, *50*, 611–615. [CrossRef]
35. Jones, C.A.; Kiniry, J.R.; Dyke, P.T. *CERES-Maize: A Simulation Model of Maize Growth and Development*; Texas A&M University Press: College Station, TX, USA, 1986.
36. Tollenaar, M.; Daynard, T.B.; Hunter, R.B. Effect of temperature on rate of leaf appearance and flowering date in maize. *Crop Sci.* **1979**, *19*, 363–366. [CrossRef]
37. Stewart, D.W.; Dwyer, L.M.; Carrigan, L.L. Phenological temperature response of maize. *Agron. J.* **1998**, *90*, 73–79. [CrossRef]
38. Tollenaar, M.; Dwyer, L. Physiology of maize. In *Crop Yield: Physiology and Processes*; Smith, D.L., Ed.; Springer: Berlin/Heidelberg, Germany, 1999; pp. 169–204.
39. Johnson, F.H.; Eyring, H.; Williams, R. The nature of enzyme inhibitions in bacterial luminescence: Sulfanilamide, urethane, temperature and pressure. *J. Cell. Comp. Physiol.* **1942**, *20*, 247–268. [CrossRef]
40. Parent, B.; Tardieu, F. Temperature responses of developmental processes have not been affected by breeding in different ecological areas for 17 crop species. *New Phytol.* **2012**, *194*, 760–774. [CrossRef] [PubMed]
41. Ali, M.; Hoque, M.; Hassan, A.; Khair, M. Photo-thermal unit requirement of wheat under different levels of irrigation. *J. Bangladesh Agric. Univ.* **2004**, *2*, 351–360. [CrossRef]
42. Lizaso, J.I.; Ruiz-Ramos, M.; Rodríguez, L.; Gabaldon-Leal, C.; Oliveira, J.A.; Lorite, I.J.; Sánchez, D.; García, E.; Rodríguez, A. Impact of high temperatures in maize: Phenology and yield components. *Field Crops Res.* **2018**, *216*, 129–140. [CrossRef]
43. Coelho, D.T.; Dale, R.F. An Energy-Crop Growth Variable and Temperature Function for Predicting Corn Growth and Development: Planting to Silking 1. *Agron. J.* **1980**, *72*, 503–510. [CrossRef]
44. Dwyer, L.M.; Stewart, D.W.; Carrigan, L.; Ma, B.; Neave, P.; Balchin, D. A general thermal index for maize. *Agron. J.* **1999**, *91*, 940–946. [CrossRef]
45. Zai, F.H.; Hamers, H.; McSharry, P.E. Evaluating the predictive accuracy of corn phenological durations in Iowa and Illinois. *Agron. J.* **2019**, *111*, 1128–1140. [CrossRef]
46. Vennam, R.R.; Ramamoorthy, P.; Poudel, S.; Reddy, K.R.; Henry, W.B.; Bheemanahalli, R. Developing functional relationships between soil moisture content and corn early-season physiology, growth, and development. *Plants* **2023**, *12*, 2471. [CrossRef]
47. Singh, G.; Narwal, S.; Rao, V.; Dahiya, D. Effect of sowing date on requirement of growing degree days, heliothermal units and photothermal units, and phenology of winter maize (*Zea mays*). *Indian J. Agric. Sci.* **1990**, *60*, 723–731.

48. Shaykewich, C. An appraisal of cereal crop phenology modelling. *J. Plant Sci.* **1995**, *75*, 329–341. [CrossRef]
49. Nelson, D.W.; Sommers, L.E. Total carbon, organic carbon, and organic matter. In *Methods of Soil Analysis: Part 3 Chemical Methods*; Sparks, D.L., Page, A.L., Helmke, P.A., Loeppert, R.H., Soltanpour, P.N., Tabatabai, M.A., Johnston, C.T., Sumner, M.E., Eds.; SSSA Book Series 5; ASA-CSSA-SSSA: Madison, WI, USA, 1996; pp. 961–1010. [CrossRef]

Disclaimer/Publisher's Note: The statements, opinions and data contained in all publications are solely those of the individual author(s) and contributor(s) and not of MDPI and/or the editor(s). MDPI and/or the editor(s) disclaim responsibility for any injury to people or property resulting from any ideas, methods, instructions or products referred to in the content.